DIFFRACTIVE JET AND CHARM PRODUCTION

N. VLASOV

Freiburg University
Physikal Institute
Hermann-Herder st. 3, 79104 Freiburg, Germany
E-mail: vlasov@mail.desy.de

The predictions of diffractive models are compared with H1 measurements of jet production cross sections in diffractive Deep Inelastic Scattering and photoproduction and with H1 and ZEUS measurements of $D^{*\pm}(2010)$ meson production in diffractive DIS.

1. Introduction

The diffractive process at HERA, characterized by a large rapidity gap in the distribution of the final-state hadrons, is considered to proceed through the exchange of an object carrying the quantum numbers of the vacuum, known as the Pomeron ($I\!P$). In the resolved-Pomeron model[1], the exchanged Pomeron acts as a source of partons, one of which interacts with the virtual photon. In an alternative view, the diffractive process at HERA can be described by the dissociation of the virtual photon into a $q\bar{q}$ or $q\bar{q}g$ state which interacts with the proton by the exchange of two gluons or, more generally, a gluon ladder with the quantum numbers of the vacuum [2,3,9].

Jet and charm production in diffractive Deep Inelastic Scattering (DIS), which have also been measured by the H1 and ZEUS collaborations [5,6,7], allow quantitative tests of the models due to the sensitivity of jet and charm production to gluon-initiated processes [8]. Final states containing heavy quarks or high transverse momentum jets are of particular interest, since the additional hard scales ensures the applicability of perturbative QCD.

Measurements of inclusive diffractive DIS at HERA have been used to extract the diffractive parton distributions (diffractive pdfs) of the proton. If QCD factorisation holds in diffractive DIS, these diffractive pdfs are universal and may be used to predict the cross sections for exclusive hard diffractive DIS processes such as jet and heavy flavour production.

2. Models of Diffractive Charm and Jet Production

2.1. *Resolved Pomeron Model*

In the resolved-Pomeron model, proposed by Ingelman and Schlein [1], the exchanged Pomeron is assumed to be a object with a partonic structure. The diffractive cross section factorises into a Pomeron flux factor, describing the probability to find a Pomeron in the proton, the Pomeron's parton density functions which specify the probability to find a given parton in the Pomeron and the interaction cross section with that parton. Within this model, open charm and jet production are produced in diffractive DIS via the boson-gluon-fusion (BGF) process, where the virtual photon interacts with a gluon from the Pomeron. The HERA measurements of the inclusive diffractive differential cross sections were found to be consistent with the resolved-Pomeron model with a Pomeron structure dominated by gluons [9,10].

A combined fit of the Pomeron parton densities to the H1 and ZEUS inclusive diffractive DIS measurements and to the ZEUS data on diffractive dijet photoproduction has been made by Alvero et al. (ACTW) [11]. The resulting diffractive parton distributions have been compared to recent ZEUS measurements of D^* meson producton in diffractive DIS [6]. Leading order (LO) and next-to-leading order (NLO) DGLAP QCD fits have been performed by H1 Collaboration to determine diffractive parton distributions [10] which were then used for comparisons with recent H1 measurements of D^* meson [7] and dijet [5] production in diffraction. The fit results have been interfaced to the program HVQDIS [12] to calculate cross sections for diffractive charm production in DIS [13] and to the program DISENT [14] to calculate cross sections for diffractive dijet production in DIS, both leading and next-to-leading order.

2.2. *Two-gluon-exchange Models*

The two-gluon-exchange models consider fluctuations of the virtual photon into $q\bar{q}$ or $q\bar{q}g$ colour dipoles that interact with the proton via colour-singlet exchange, the simplest form of which is a pair of gluons [15,16,17]. The virtual-photon fluctuations into $c\bar{c}$ and $c\bar{c}g$ states can lead to diffractive open-charm production. At high $x_{I\!P}$ values, quark exchanges are expected to become significant, implying that the two-gluon-exchange calculations are expected to be valid only at low $x_{I\!P}$ values ($x_{I\!P} < 0.01$). In the calculations [3,18,19,20], used here, the cross section for two-gluon exchange is related to the square of the unintegrated gluon distribution of the proton which depends on the gluon transverse momentum, k_T, relative to the proton direction. In the "saturation" model [20,21], the calculation of the $q\bar{q}g$ cross section is performed under the assumption of strong k_T ordering of the final-state partons, which corresponds to $k_T^{(g)} \ll k_T^{(q,\bar{q})}$. The parameters of the model were tuned to describe the total photon-proton cross section measured at HERA. Alternatively, in the model of Bartels et al. [3,18,19], configurations without strong k_T ordering are included in the $q\bar{q}g$ cross-section calculation and the minimum value for the final-state-gluon transverse momentum, $k_{T,g}^{\text{cut}}$, is a free parameter which has been tuned to describe the H1 dijet cross sections [5]. The sum of the $q\bar{q}$ and $q\bar{q}g$ contributions in the saturation model and the model of Bartels et al. are hereafter referred to as SATRAP and BJLW, respectively.

3. Diffractive Jets and Charm in DIS

In this section the recent H1 and ZEUS measurements of dijets and D^* meson production in diffractive DIS are compared with the different models.

In diffractive DIS, a proton with virtuality Q^2 emitted from the beam electron interacts with the proton, which loses only a small fraction $x_{I\!P}$ of its incident momentum and stays intact (or dissociates into a small mass system Y). The longitudinal momentum fraction of the parton entering the hard scattering process relative to the diffractive exchange is labelled $z_{I\!P}$ (equivalent to β at LO). In the hard scattering process, a pair of high transverse momentum (p_T) jets or heavy quarks is produced. The photon-proton centre-of-mass energy is W, which is related to the inelasticity y via $ys = Q^2 + W^2$, where s is the ep centre-of-mass energy squared. The invariant mass of the diffractively produced system X is M_X, and the invariant mass of the two partons emerging from the hard sub-process is given by $\sqrt{\hat{s}} = M_{12}$.

3.1. *Diffractive Dijets in DIS*

The H1 Collaboration has measured differential cross sections for the diffractive production of dijets in DIS [5]. The jets are found using the CDF cone algorithm with cone radius $R = 1$. The kinematic range of the measurement is $4 < Q^2 < 80$ GeV^2, $0.1 < y < 0.7$, $x_{I\!P} < 0.05$, $|t| < 1.0$ GeV^2 and $M_Y < 1.6$ GeV. The transverse momenta and pseudorapidities of the two jets, which are searched for in the hadronic centre-of-mass frame, are required to satisfy $p^*_{T,jet} > 4$ GeV and $-3 < \eta^*_{jet} < 0$, respectively.

To facilitate a comparison of the cross sections with NLO calculations, the data were corrected to the kinematic region where the transverse momentum of the first (second) jet is $p^*_{T,jet} > 5(4)$ GeV, as the next-to-leading order dijets cross sections are not reliable in regions of phase space where the two jets have the same transverse momentum [22].

To calculate diffractive dijet cross sections to NLO in QCD, the DISENT program was used. Since the calculations refer to partonic jets, whereas the measurements refer to hadronic jets, the NLO calculations have been corrected for the hadronisation effects.

In Fig. 1, the differential cross sections for dijet production in diffractive DIS are presented as functions of $z_{I\!P}^{jets}$, Q^2, W, $log_{10}x_{I\!P}$ and the average pseudorapidity $\langle\eta\rangle_{lab}^{jets}$ of the jets. The data are compared with leading and next-to-leading order calculations using DISENT interfaced to the H1 diffractive pdf's [10]. The uncertainty on the NLO calculations was estimated by varying the renormalisation scale $\mu_R^2 = p_T^2$ by factors of 1/4 and 4 and the hadronisation corrections. The NLO calculation provides within the theoretical and experimental uncertainties a reasonable description of the shapes and normalisations of the measured cross sections.

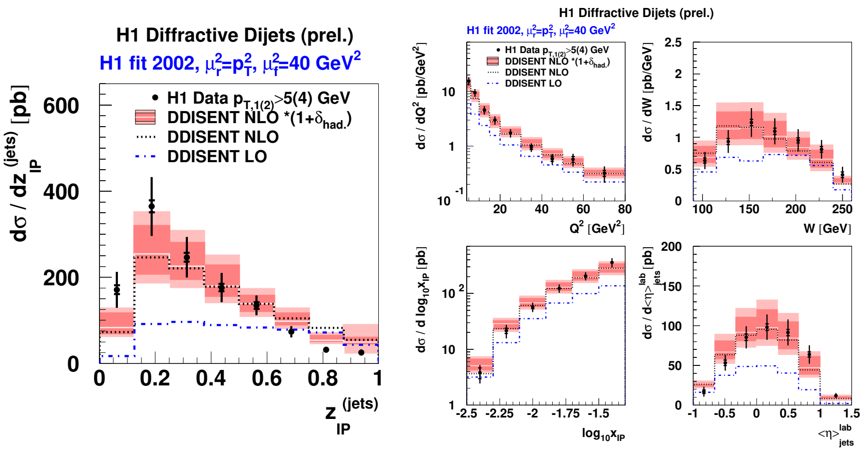

Figure 1. Differential cross sections for dijet production in diffractive DIS (dots) as a function of $z_{I\!P}^{jets}$, Q^2, W, $log_{10}x_{I\!P}$ and $\langle\eta\rangle_{lab}^{jets}$. The data are compared with predictions from NLO calculations.

In Fig. 2, the differential dijet cross sections in the region $x_{I\!P} < 0.01$ are compared with the predictions of the Saturation, BJLW and Resolved Pomeron (Pomeron parametrisation 'h1 fit2' [7]) models. The $P_{T,rem}^{(I\!P)}$ variable measures the transverse momentum of all hadronic final state particles in the Pomeron hemisphere of the $\gamma^* I\!P$ centre-of-mass frame which do not belong to the two highest p_T^* jets.

The saturation model is able to reproduce the shapes of the measured cross sections, although the overall predicted dijet rate is too low by a factor of about 2. In the BJLW model, the contribution from $q\bar{q}$ states is negligible and the dominant contribution comes from $q\bar{q}g$ final states. The normalisation of the BJLW model for $q\bar{q}g$ production can be controlled by tuning the lower limit on the transverse momentum of the gluon, $p_{T,g}^{cut}$, in the calculations. If this limit is set to 1.5 GeV, the total cross section for dijet production with $x_{I\!P} < 0.01$ is in agreement with the model [5].

In Fig. 2, the Resolved Pomeron model gives a good description of all observables, including the $P_{T,rem}^{(I\!P)}$ distribution. The good description of the $P_{T,rem}^{(I\!P)}$ distribution by both the Resolved Pomeron and the BJLW models indicates that the present data are not able to discriminate between models with a soft "remnant“ and those with a third high-p_T parton.

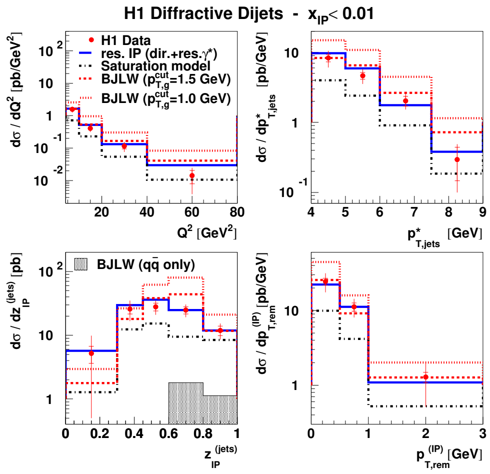

Figure 2. Differential cross sections for dijet production in diffractive DIS (dots), shown as functions of Q^2, $p_{T,jets}^*$, $z_{I\!P}^{jets}$ and $P_{T,rem}^{(I\!P)}$. The data are compared with different models.

3.2. *Diffractive D^* in DIS*

The ZEUS Collaboration has measured charm production in diffractive DIS [6]. Figure 3 shows the differential cross sections measured in the kinematic range $1.5 < Q^2 < 200$ GeV^2, $0.02 < y < 0.7$, $\beta < 0.8$, $p_T(D^*) > 1.5$ GeV and $|\eta(D^*)| < 1.5$ as functions of β, $\log(\beta)$, $\log(Q^2)$ and W for $x_{I\!P} < 0.035$ and as functions of $p_T(D^*)$, $\eta(D^*)$, $\log(M_X^2)$ and β for $x_{I\!P} < 0.01$. The data are compared with the ACTW NLO predictions, calculated with the gluon-dominated fit B, the SATRAP predictions and the BJLW predictions (only for $x_{I\!P} < 0.01$).

The two-gluon-exchange BJLW model predictions, obtained with the requirement that $k_{T,g}^{\rm cut} = 1.5$ GeV, describe the differential cross sections in the range $x_{I\!P} < 0.01$ both in shape and normalisation. The saturation model (SATRAP) predictions reproduce the shapes and the normalisations of the differential cross sections measured in both $x_{I\!P}$ ranges. The ACTW NLO predictions, obtained with the gluon-dominated fit B, describe the data reasonably well in both $x_{I\!P}$ ranges.

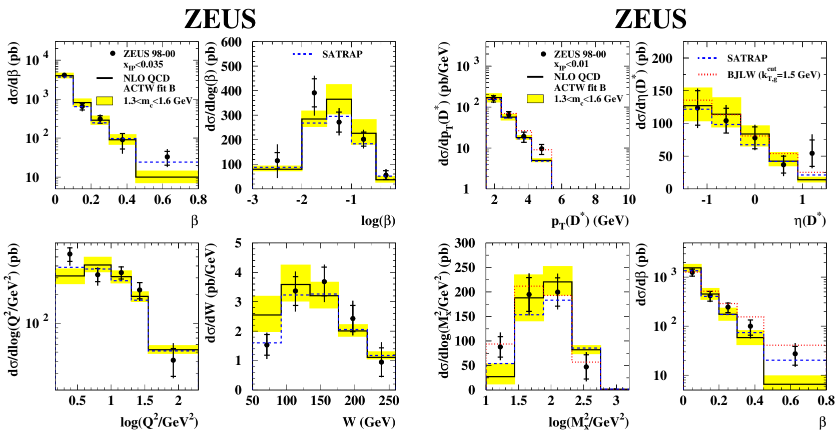

Figure 3. Differential cross sections for diffractive D^* production (dots) compared with different models (see text). The inner error bars indicate the statistical uncertainties, while the outer ones correspond to the statistical and systematic uncertainties added in quadrature. The shaded area shows the effect of varying the charm-quark mass in the ACTW NLO prediction.

Fig. 4 shows the quantity $x_{I\!P} F_2^{D(3),c\bar{c}}$ measured by ZEUS Collaboration [6] where $F_2^{D(3),c\bar{c}}$ is the open-charm contribution to the diffractive proton structure function. It is shown as a function of $\log(\beta)$ for different values of Q^2 and $x_{I\!P}$. In all cases, $x_{I\!P} F_2^{D(3),c\bar{c}}$ rises as β decreases. The curves show the predictions obtained from the ACTW NLO calculations based on fits B, D and SG [11]. The fit B prediction generally agrees with the data. The fit

D (SG) prediction overestimates (underestimates) the measured $x_{I\!P} F_2^{D(3),c\bar{c}}$ at low β.

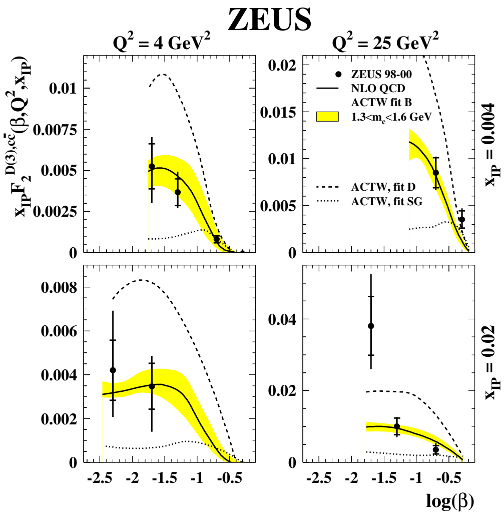

Figure 4. The measured charm contribution to the diffractive structure function of the proton multiplied by $x_{I\!P}$, $x_{I\!P} F_2^{D(3),c\bar{c}}$, as a function of β for different values of Q^2 and $x_{I\!P}$ (dots). The inner error bars indicate the statistical uncertainties, while the outer ones correspond to the statistical and systematic uncertainties added in quadrature. The shaded area shows the effect of varying the charm-quark mass in the ACTW NLO prediction.

Differential cross sections for D^* production in diffractive DIS have also been measured by H1[7]. The kinematic range of the data corresponds to $2 < Q^2 < 100$ GeV^2, $0.05 < y < 0.7$, $x_{I\!P} < 0.04$, $|t| < 1$ GeV^2, $M_Y < 1.6$ GeV, $p_T(D^*) > 2$ GeV and $|\eta(D^*)| < 1.5$.

Figure 5 shows the differential cross sections as functions of $\log(Q^2)$, $p_T(D^*)$, $\eta(D^*)$ and $x_{I\!P}$. The data are compared with the leading and next-to-leading order calculations from the diffractive version of HVQDIS, interfaced to the H1 diffractive pdf's [10]. Within the experimental and theoretical uncertainties, good agreement is observed between the data and NLO calculations.

3.3. *Dijets in Diffractive Photoproduction*

As shown in Sec. 3.1, diffractive dijet production in DIS is in good agreement with the QCD fits to inclusive diffractive data. However, applying

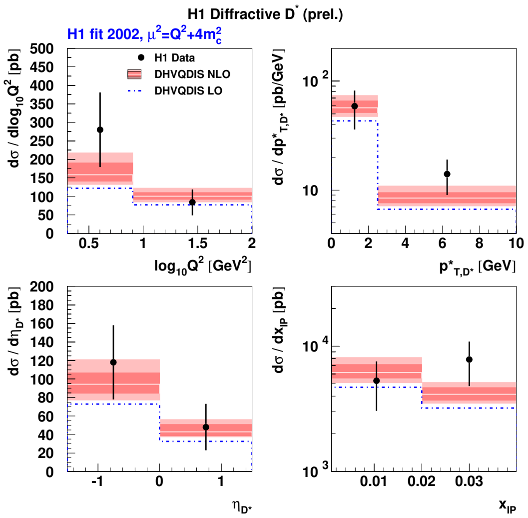

Figure 5. Differential cross sections for diffractive D^* production (dots) compared with NLO calculations. The error bars of the data correspond to the sum of statistical and systematic uncertainties, added in quadrature. The inner error band represents the renormalisation scale uncertainity, while the outer band also includes the uncertainty in the hadronization corrections, added lineary.

the diffractive parton densities to predict diffractive jet production at the Tevatron, leads to an overestimation of the observed rate by one order of magnitude [23]. This discrepancy has been attributed to the presence of the additional beam hadron remnant in $p\bar{p}$ collisions which leads to secondary interactions and a break-down of factorisation. The suppression cannot be calculated perturbatively and has been parametrised in various ways [24,25,26].

The transition from DIS to hadron-hadron scattering has been studied with the H1 detector in photoproduction regime, where the beam lepton emits a quasi-real photon which interacts with the proton [27]. Processes in which the photon is first resolved into partons which then initiate the hard scattering resemble hadron-hadron scattering. Via the resolved photon process in hard photoproduction, hadronic final states are accessible, which are present in the equivalent $p\bar{p}$ collisions but not in DIS.

Dijet events are identified using the inclusive k_T cluster algorithm [27]. Fig. 6 shows the differential cross sections with respect to $z_{\mathbb{P}}^{jets}$ and the estimator x_γ^{jets} of the fractional photon momentum taking part in the hard scattering. The cross sections are given at hadron level and correspond to the kinematic range $Q^2 < 0.01$ GeV^2, $165 < W < 240$ GeV, $x_{I\!P} < 0.03$, $E_T^{jet1} > 5$ GeV and $E_T^{jet2} > 4$ GeV. The H1 2002 fit [10] gives a good description of the diffractive dijet photoproduction. The contribution from the direct photon process ($x_\gamma^{true} = 1$) is indicated by the hatched histogram. The sum of resolved and direct photon processes in the model gives a good description of the data both in normalisation and in shape throughout the x_γ^{jets} range. Hence there is no evidence for any suppression of the diffractive cross section in the region dominated by resolved photons, as might be expected on the basis of data from the Tevatron [23] or phenomenological models [24,25,26].

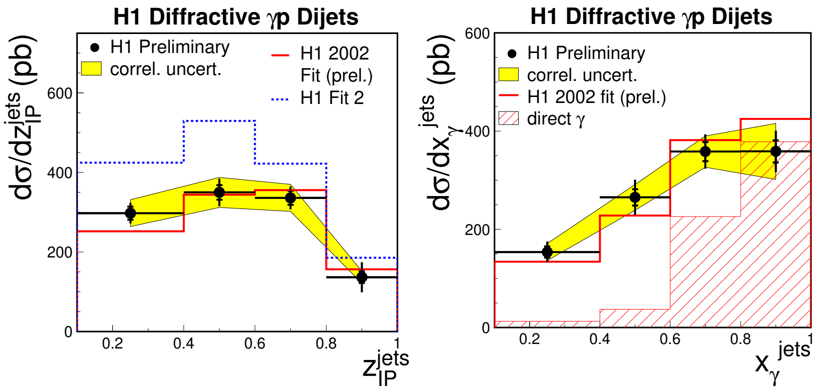

Figure 6. Differential cross sections in $z_{I\!P}^{jets}$ and x_γ^{jets} in diffractive photoproduction (dots). The inner error bars represent the statistical errors and the outer error bars the quadratic sum of the statistical and uncorrelated systematic errors.

References

1. G. Ingelman and P.E. Schlein, *Phys. Lett.* **B152**, 256 (1985).
2. H. Lotter, *Phys. Lett.* **B406**, 171 (1997).
3. J. Bartels, H. Jung and M. Wüsthoff, *Eur. Phys. J.* **C11**, 111 (1999).
4. E.M. Levin et al., *Z. Phys.* **C74**, 671 (1997).
5. H1 Collab., Adloff et al., *Eur. Phys. J.* **C20**, 29 (2001).
6. ZEUS Collab., S. Chekanov et al., *Nucl. Phys.* **B672**, 3-35 (2003).
7. H1 Collab., Adloff et al., *Phys. Lett.* **B520**, 191 (2001).
8. M.F. McDermott and G. Briskin, *Proc. Workshop on Future Physics at HERA*, G. Ingelman, A. De Roeck and R. Klanner (eds.), Vol.2, p.691, Hamburg, Germany, DESY (1996).
9. H1 Collab., C. Adloff et al., *Z. Phys.* **C76**, 613 (1997).
10. H1 Collaboration, *Measurement and NLO DGLAP QCD Interpretation of Diffractive Deep-Inelastic Scattering at HERA*, paper **980** submitted to the

31st Intl. Conference on High Energy Physics, ICHEP2002, Amsterdam (2002).
(http://www-h1.desy.de/h1/www/publications/htmlsplit/H1prelim-02-012.long.html)
11. L. Alvero et al., *Phys. Rev.* **D59**, 074022 (1999).
12. B.W. Harris and J. Smith, *Phys. Rev.* **D57**, 2806 (1998).
13. L. Alvero, J.C. Collins and J.J. Whitmore, [hep-ph/9806340].
14. S. Catani, M.H. Seymour, *Nucl. Phys.* **B485**, 29 (1997).
15. F.E. Low, *Phys. Rev.* **D12**, 163 (1975).
16. S. Nussinov, *Phys. Rev. Lett.* **34**, 1286 (1975).
17. S. Nussinov, *Phys. Rev.* **D14**, 246 (1976).
18. J. Bartels, H. Lotter and M. Wüsthoff, *Phys. Lett.* **B379**, 239 (1996).
19. J. Bartels, H. Jung and A. Kyrieleis, *Eur. Phys. J.* **C24**, 555 (2002).
20. K. Golec-Biernat and M. Wüsthoff, *Phys. Rev.* **D59**, 014017 (1999).
21. H. Kowalski, *Proc. Workshop on New Trends in HERA Physics*, G. Grindhammer, B.A. Kniehl and G. Kramer (eds.), pp. 361-380 (1999), available on http://www-library.desy.de/conf/ringberg99.html
22. H1 Collaboration, *Comparison at NLO between Predictions from QCD Fits to F_2^D and Diffractive Final State Observables at HERA*, paper **113** submitted to the Intl. Europhysics Conference on High Energy Physics, EPS2003, Aachen (2003).
(http://www-h1.desy.de/h1/www/publications/htmlsplit/H1prelim-03-015.long.html)
23. CDF Collaboration, T. Affolder et al., *Phys. Rev. Lett.* **84**, 5043 (2000).
24. E. Gotsman, E. Levin and U. Maor, *Phys. Lett.* **B438**, 229 (1998).
25. B. Cox, J. Forshaw and L. Lönnblad, [hep-ph/9908464].
26. A. Kaidalov, V. Khoze, A. Martin and M. Ryskin, [hep-ph/0306134].
27. H1 Collaboration, *Dijets in Diffractive Photoproduction at HERA*, paper **087** submitted to the Intl. Europhysics Conference on High Energy Physics, EPS2003, Aachen (2003).
(http://www-h1.desy.de/h1/www/publications/htmlsplit/H1prelim-02-113.long.html)